Available online at www.sciencedirect.com
ScienceDirect
Ceramics International 38 (2012) 695–700
CERAMICS INTERNATIONAL
www.elsevier.com/locate/ceramint

Influence of reduced substrate shunting current on cell performance in integrated planar solid oxide fuel cells

Keonseok Oh [a,1], Joosun Kim [b,**], Sun Hee Choi [b], Daehee Lee [a], Jooho Moon [a,*]

[a] Department of Materials Science and Engineering, Yonsei University, Seoul 120-749, Republic of Korea
[b] High Temperature Energy Materials Research Center, KIST, Seoul 136-791, Republic of Korea

Received 17 May 2011; received in revised form 19 July 2011; accepted 25 July 2011
Available online 30th July 2011

Abstract

Two-cell arrayed integrated planar solid oxide fuel cells (IP-SOFCs) were fabricated using a robo-dispensing method. Special emphasis was placed on the influence of reduced shunting current on cell performance. The resistivity of the substrate increased according to a mixture rule of composites by adding Al_2O_3 into the substrate of partially stabilized zirconia (PSZ). This strategy, which reduces shunting current through the substrate, enhances the power output. When the amount of Al_2O_3 added was more than 26 vol%, however, the Ni anode migrated into the PSZ substrate to react with Al_2O_3, which led to performance degradation. In the case of the two-cell arrayed IP-SOFC with a 20 vol%-Al_2O_3 added to the PSZ substrate, a reduced shunting current loss improved the power density by 30% compared to that of the Al_2O_3-free substrate.

Keywords: Al_2O_3; Integrated planar SOFC; Substrate resistivity; Shunting current; Robo-dispensing

1. Introduction

Integrated planar solid oxide fuel cells (IP-SOFCs) have been studied since they were first demonstration by Rolls-Royce [1,2]. They are essentially a cross-over between tubular and planar geometries, designed to exploit the thermal compliance properties of planar/monolithic SOFCs and the low-cost component fabrication of tubular SOFCs [3,4]. The unique design concept of IP-SOFCs offers several advantages over other fuel cells. First, IP-SOFCs have much shorter interspacing between unit cells and narrower electrode width than those of the established planar or tubular types. These allow easy cell integration with minimal resistance losses, which makes them suitable as mobile power sources that can deliver high current density and high voltage per unit area [5,6]. Secondly, the cells are fabricated on a planar or a flat tube substrate using a simple colloidal ceramic processing method. Thereby, thin electrolyte deposition and gas-tight sealing between the fuel and air chambers are readily accomplished.

The performance of an IP-SOFC is significantly influenced by the cell dimensions. Lai and Barnett demonstrated that high power densities could be achieved by reducing the cell length, L_{cell}, below the value of ~1 cm [2,3]. Further, Pillai et al. reported that a short repeat period of 2.4 mm and a small cell length of 1.3 mm improved cell performance [7]. The substrate that supports the cells should not only be compatible with the cell materials at high temperatures, but it should also maintain good mechanical strength and have sufficient porosity for fuel transport. Partially stabilized zirconia (PSZ) is usually utilized for IP-SOFCs because of its good chemical stability and thermal expansion match with those of SOFC materials. However, the ionic conductivity associated with PSZ can induce leakage current between two neighboring anodes, typically called shunting current.

In this study, we suggest that a simple addition of Al_2O_3 to the substrate can improve the cell performance and show that its impact improves performance beyond the theoretical expectation. We have fabricated two-cell serially connected IP-SOFCs using a robo-dispensing process [8]. We investigated the influence of reduced shunting current on the cell power by utilizing the PSZ substrate whose conductivity is reduced

* Corresponding author. Tel.: +82 2 2123 2855; fax: +82 2 312 5375.
** Corresponding author. Tel.: +82 2 958 5528; fax: +82 2 958 5529.
E-mail addresses: joosun@kist.re.kr (J. Kim), jmoon@yonsei.ac.kr (J. Moon).
[1] Current address: SB LiMotive Co., Ltd., Cell R&D Team, Suwon 443-731, Republic of Korea.

0272-8842/$36.00
doi:10.1016/j.ceramint.2011.07.058

through the addition of an insulating phase. Reducing the shunting current brings about an improvement in the power density, even for operation temperatures of 800 °C and for cell repeat periods >2.0 mm.

2. Experimental

Commercially available 3 mol%-Y_2O_3-doped ZrO_2 (PSZ, TZ3YS, Tosoh Co., Japan) powder was used to prepare the substrate. To obtain a microporous substrate, a resin containing PSZ was granulated using a liquid condensation process (LCP) [9]. For control of ionic conductivity, Al_2O_3 (AKP30, Sumitomo Chem. Co., Japan) was mixed with PSZ particles at varying concentrations of 13, 20 and 26 vol% prior to granulation. Granules were uni-axially pressed into disc-shaped pellets of 35 mm diameter at a pressure of 7 MPa, followed by sintering at 1350 °C for 3 h in air. The porosity of the sintered substrate was measured using mercury porosimetry (AutoPore IV, Micromeritics, USA), and gas permeability was determined using a perm porometer (Porous Materials Inc., USA). Four-point flexural strengths were also measured using a universal test machine (4467, Instron Co., USA). The electrical conductivities of Al_2O_3-added PSZ substrates were measured using a four-probe method with a digital multimeter (2000 & 2430, Keithley).

The paste for each compartment of the fuel cell, i.e., anode, electrolyte, and cathode, was formulated by mixing each corresponding commercial powder, ethyl cellulose and the appropriate dispersing agent in α-terpineol solvent. NiO (Sumitomo Chem. Co., Japan) and 8 mol%-Y_2O_3-doped ZrO_2 (YSZ, TZ8Y, Tosoh Co., Japan) powder in a weight ratio of 6:4 were used as anode paste, YSZ was used as the electrolyte, and $(La_{0.7}Sr_{0.3})_{0.95}MnO_3$ (LSM, Seimi Chem. Co., Japan) was used as the cathode. Each formulated paste had a fixed solid loading of 15 vol% and was mixed using a planetary mill (Pulverisette 5, Fritsch Co., Germany).

Electrodes and electrolyte pastes were dispensed through a cylindrical nozzle 0.21 mm in diameter under an air pressure of 0.1 Torr onto the moving plate at a speed of 1.22 mm/s using a computer-controlled robo-dispensing machine (ML-505GX, Musashi, Japan) [8]. The anode paste was dispensed onto the porous substrate and dried at 55 °C for 1 h. The electrolyte paste was then dispensed onto the top of the anode with an offset distance of 0.1 mm, covering 90% of the anode area. The NiO-YSZ/YSZ multilayer on the Al_2O_3-added PSZ substrate was co-fired at 1350 °C for 1 h in air. Similarly, the cathode layer was dispensed onto the top of the electrolyte and then sintered at 1200 °C for 1 h in air. The anode area not covered by the electrolyte was sealed with a glass paste, and an Au interconnector (8881-B, ESL Inc., USA) paste was also dispensed between the anode of one cell and the cathode of the next. The dispensed microstructures were observed using optical microscopy (DMLM, Leica) and scanning electron microscopy (FEIXL-30, FEG, Philips). The compositional distribution across the compartment interfaces within a cell was determined using energy-dispersive X-ray spectroscopy (EDS) after the performance measurements.

The fabricated IP-SOFC cell was placed into the hot zone of a vertical furnace, and Au wires were employed as current collectors for linear anode and cathode electrodes at both ends. The current–voltage and current–power characteristics were measured with an SOFC test station (SAT890, Toyo, Japan) at 800 °C. Air was used as an oxidant, and 3% moisturized hydrogen gas (97% H_2 + 3% H_2O) at a flow rate of 100 sccm was used as a fuel.

3. Results and discussion

Fig. 1 shows the schematic design of our IP-SOFC cell direct-written onto a porous substrate using a robo-dispensing process. The unit cell consists of aligned multi-components, i.e., anode, electrolyte, cathode, and interconnect lines with a

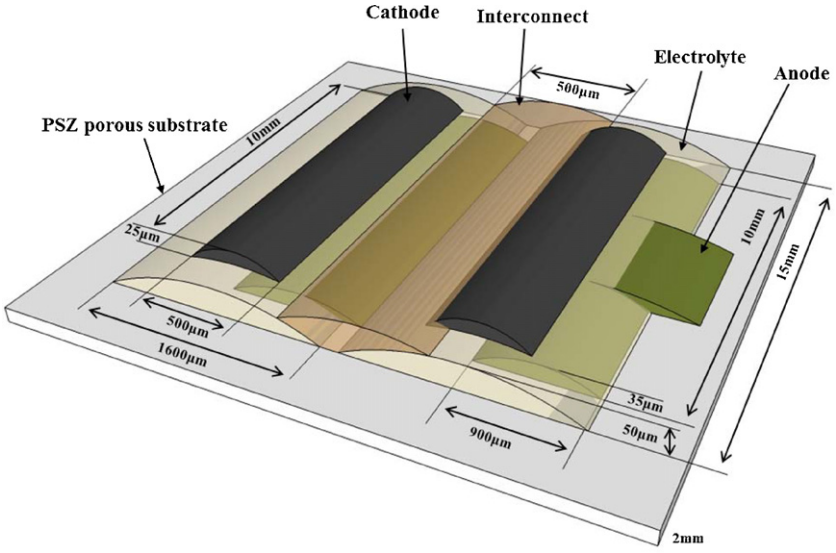

Fig. 1. Schematic diagram of the two-cell serially connected IP-SOFC.

Table 1
Physical and electrochemical properties of two-cell arrayed IP-SOFCs.

Sample	Substrate			Cell			
	Al_2O_3 content (vol%)	Porosity (%)	Resistivity (Ω cm)	Cell-to-cell distance (mm)	ASR[a] (Ω cm^2)	OCV[b] (V)	Maximum power density (mW/cm^2) @800 °C
IP00A05	0	37	150	0.5	2.76	1.64	240
IP00A10	0	37	150	1	2.11	1.86	350
IP00A30	0	37	150	3	2.79	1.87	300
IP13A10	13	24	200	1	1.75	1.89	408
IP20A05	20	28	250	0.5	2.06	1.88	360
IP20A10	20	28	250	1	1.64	1.89	455
IP20A30	20	28	250	3	1.77	1.77	388
IP26A10	26	30	370	1	1.76	1.77	393

IP*xx*A*yy*: sample identification in which *xx* denotes Al_2O_3 content and *yy* represents cell-to-cell distance.
[a] ASR: area specific resistance.
[b] OCV: open cell voltage.

fixed offset distance. The rheological behavior of the paste (i.e., the spreading and wetting characteristics of the paste extruded from the nozzle tip) determined the subsequent microstructure of the cell. Therefore, the amounts of binder and dispersant for each paste need to be optimized in order to produce SOFCs with desirable microstructures and dimensions. The apparent viscosity of the optimized paste was in the range of 40,000–45,000 mPa s at a shear rate of 10 s^{-1} for the electrodes and 5000–8000 mPa s for the electrolyte. The anode and the cathode layers were porous and showed layer thicknesses of about 30 μm and 20 μm, respectively, whereas the 15-μm-thick YSZ electrolyte was fully dense. All of the laminated layers exhibited good adhesion to one other, with no evidence of delamination or defect generation.

The porous supporting substrate plays important roles in the IP-SOFCs. It should not only have good thermal and mechanical stabilities, but should also permit sufficient transport of the fuel gas to the anodes. Furthermore, the substrate needs to be an insulator so that the conduction through the substrate in contact with the anode, i.e., shunting current, does not lead to a performance loss. The addition of Al_2O_3 to the PSZ substrate has a beneficial effect on the porosity, as shown in Table 1. As the amount of Al_2O_3 was increased, the porosity of the substrate was increased from 24 to 30% without significant strength degradation (~100 MPa). However, the porosities of the Al_2O_3-added substrate were lower than those of the Al_2O_3-free substrate. Both the fabricated pure PSZ and Al_2O_3-added PSZ substrates had a uniform microstructure composed of a fine and narrow distribution of pores about 1 μm in diameter. The permeabilities of the sintered substrates were greater than 3.69×10^{-12} m^2, indicating that gas permeation through the substrate was comparable to 600 cc/m when the pressure difference was ~30 psi [8]. Considering the feeding rate of fuel gas during operation, our substrates retained sufficient porosity through which the fuel gas could be supplied without any resistance for gas diffusion.

Addition of Al_2O_3 brings about a beneficial effect in terms of the cell performance. PSZ is not an insulator but retains some ionic conductivity. The electrical conductivities of the substrates decreased with increased addition of Al_2O_3, as shown in Fig. 2. The present samples can be considered as a composite comprised of the conducting phase (PSZ) and the insulating phases of Al_2O_3 and the pores. According to the work of Eucken, the electrical conductivity of such a two-phase composite can be estimated [10]. If the continuous phase (PSZ) has a conductivity σ_c and the dispersed phase (pore and Al_2O_3) has a conductivity σ_d, the resulting conductivity of the mixture, σ_m, is given by:

$$\sigma_m = \sigma_c \frac{1 + 2\nu_d(1 - \sigma_c/\sigma_d)/(2\sigma_c/\sigma_d + 1)}{1 - \nu_d(1 - \sigma_c/\sigma_d)/(\sigma_c/\sigma_d + 1)}$$

where ν_d is the volume fraction of the dispersed phase, which corresponds to the summation of the volume fractions of pore (ν_p) and Al_2O_3 (ν_a). As shown in Fig. 2, the measured conductivities of the substrates matched well with the theoretically estimated values, which demonstrates that the conductivity of

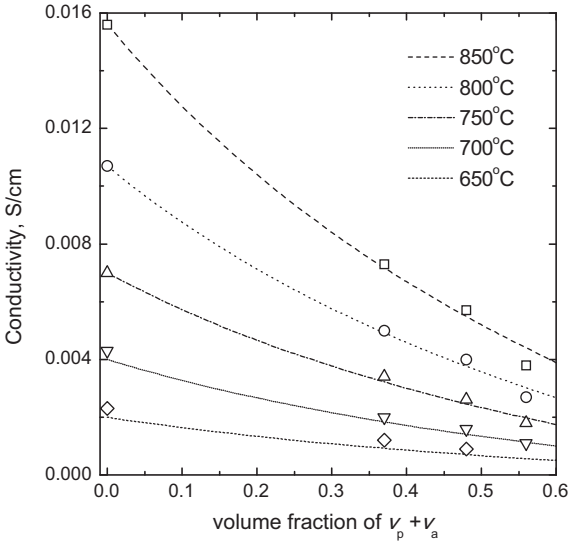

Fig. 2. Electrical conductivity of the Al_2O_3-added porous PSZ substrates as a function of the Al_2O_3 content and pore volume at various temperatures. The dashed lines represent theoretical values of the conductivity according to Eucken.

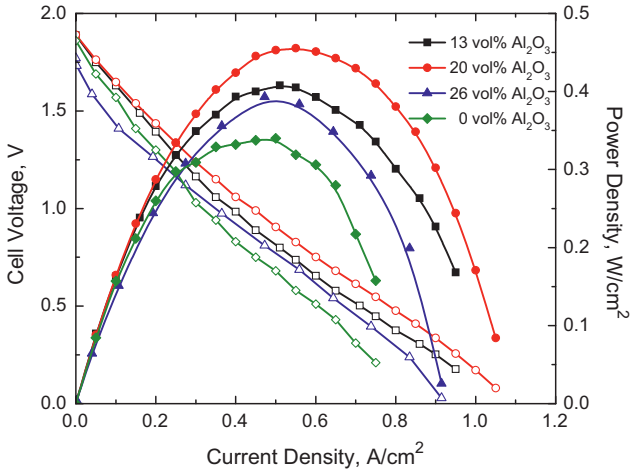

Fig. 3. Discharge characteristics of the two-cell serially connected IP-SOFCs at 800 °C on PSZ substrates with varying amounts of Al_2O_3. Cell-to-cell interspacing was fixed to 1 mm.

the PSZ substrate can be controlled by addition of Al_2O_3 in a two-phase composite regime.

Fig. 3 shows current–voltage and current–power characteristics of two-cell serially integrated planar SOFCs on composite substrates with different Al_2O_3 contents at 800 °C. Power densities were calculated using the cell active area defined by the overlapped area between the anode and the cathode [2]. Regardless of the added alumina content, the open circuit voltage (OCV) of the cells was in the range of 1.8–1.9 V, which was slightly lower than the theoretical value of 2.2 V. The reduced OCV likely results from gas leakage through the imperfect sealing of porous supports by glass pastes and Au interconnects [2,8]. Power densities for the cells on the substrate containing Al_2O_3 were enhanced compared to that on the pure PSZ substrate, although the improvement was not directly proportional to the added amount, showing a maximum value (455 mW/cm^2) at a 20 vol% Al_2O_3 addition. Further addition reduced the cell performance (393 mW/cm^2).

Variation in the performance can be understood in terms of the substrate effect. According to Lai et al.'s equation [2], shunting current has a reciprocal relation with the specific resistivity of the substrate. In this regard, the increase in the specific resistivity of the substrate would reduce the shunting current, which leads to an improved power density. Contrary to our observation, Lai and Barnett demonstrated that the effect of shunting current does not substantially affect the cell performance, causing at most a 5–6% degradation in terms of the maximum power density [3]. For the cells with a cell-to-cell distance of 1 mm, the power density at 800 °C increased from 350 mW/cm^2 to 455 mW/cm^2 when 20 vol% Al_2O_3 was added to pure PSZ substrate, which corresponds to a 30% enhancement. The area-specific resistances (ASR) for the cell were inversely correlated to the resistivity of the substrate and, in turn, the cell power density. This observation indicates that the reduced shunting currents induced by the increased resistivity of the substrate can deliver more current at the same overpotential level, manifested by the enhanced power output. The shunting current had a more substantial impact on our IP-SOFCs than it did in the previous estimation by Lai et al.

Addition of 26 vol% Al_2O_3 to the substrate further increased the substrate resistivity from 250 to 370 Ω cm, but the cell power was reduced from 455 to 393 mW/cm^2. In order to understand the reason for the deterioration, a compositional analysis across the substrate-anode interface was performed. As

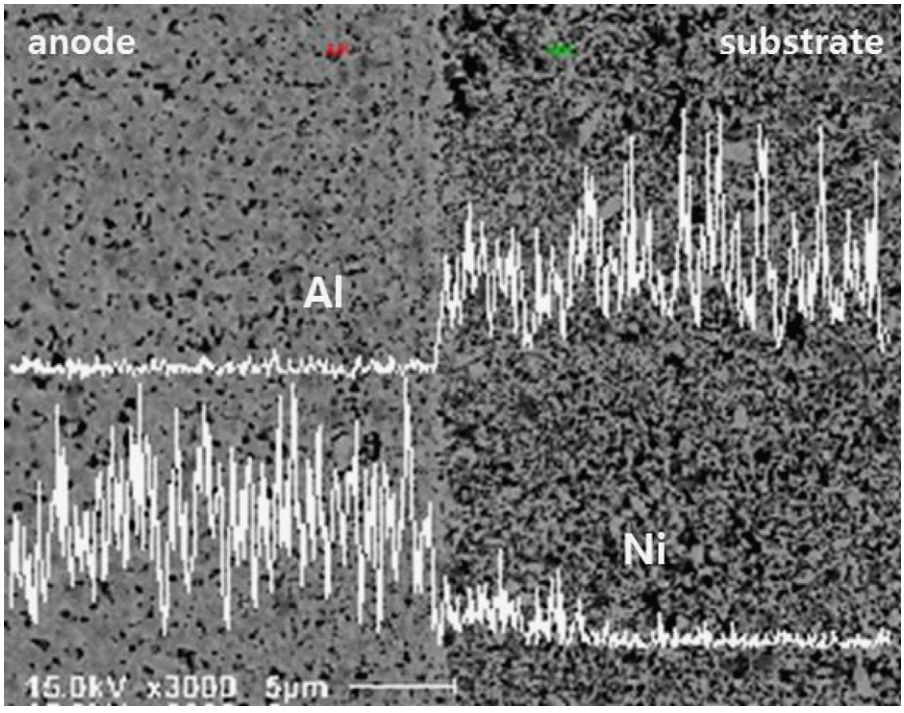

Fig. 4. Compositional profiles of Al and Ni across the anode-substrate interface of IP-SOFC.

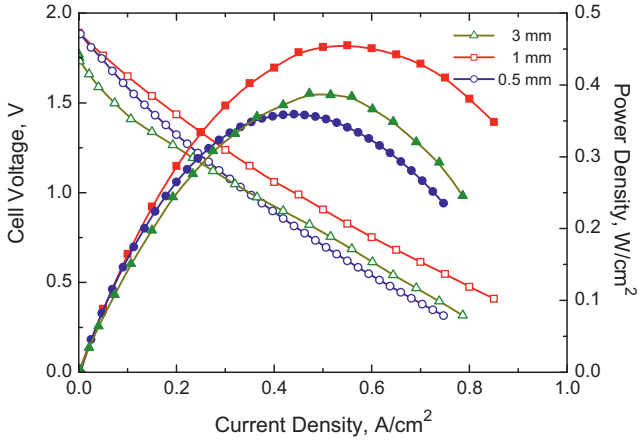

Fig. 5. Discharge characteristics of the two-cell serially connected IP-SOFCs with different cell-to-cell interspacing at 800 °C. The cells were constructed on the 20 vol% Al_2O_3-added PSZ substrate.

shown in Fig. 4, Ni diffused into the substrate layer. It is likely that Ni diffusion results in the formation of $NiAl_2O_4$ via reaction between Al_2O_3 and Ni, as reported in the conventional SOFCs [11]. In particular, *I–V* characteristics of the cell on the 26 vol% Al_2O_3-added substrate showed a significant voltage drop due to activation polarization at the lower current density compared to those in cells on the substrates containing lower alumina amounts. It is expected that increased voltage loss results from the reduced triple phase boundary (TPB) site density for catalytic reactions in the electrodes [12]. The formation of $NiAl_2O_4$ would result in occupation of the catalytically active sites on the Ni anode, and since $NiAl_2O_4$ is catalytically inert toward the oxidation of hydrogen, this deteriorates the cell performance [11]. We performed a separate experiment in which the powder mixture of Al_2O_3, NiO, and PSZ was heat-treated at the same temperature as the cell operation condition which corresponds to 800 °C in H_2 atmosphere. The phase formation of $NiAl_2O_4$ was confirmed by X-ray analysis. However, we did not observe any $NiAl_2O_4$ in the fabricated substrates, which was due to the detection limit of the instrument.

In addition, we might correlate the Ni migration with the amount of Al_2O_3 addition in PSZ substrates. The critical amount of dispersed Al_2O_3 phase for percolation in the PSZ matrix might be greater than 20 vol% [13]. Therefore, in the case of the 26 vol% of Al_2O_3-added substrate, diffusion of Ni through the substrate may occur because the Al_2O_3 continuous network provides a diffusion path across entire the substrate, which results in loss of Ni catalyst from anodes. Because reaction with Ni and ZrO_2 is negligible at SOFC operating temperatures, only Ni migration through the Al_2O_3 phase is likely to be a valid assumption. Thus, Al_2O_3 addition into the substrate should be less than the critical amount required for percolation, which prevents significant migration of Ni into the substrate.

Fig. 5 shows the performances of the cells fabricated with different cell-to-cell gap distances on the 20 vol% Al_2O_3-added PSZ substrate. The cell power density reached a maximum when the cell-to-cell gap distance was 1 mm. Narrowing the cell-to-cell gap distance can reduce the shunting current, as demonstrated by Lai and Barnett [3]. They noted that a shorter gap distance narrow the spaces of the equi-potential lines between the anode of one cell and the neighboring anode, which induces a higher shunting current density. Therefore, the ASR for the cell with 1 mm distance had a lower value than that with 0.5 mm for the same voltage output level (see Table 1). Increasing the cell-to-cell gap distance beyond the optimum value also increased the ASR and decreased the power density since a wider gap distance reduced the active electrode-areal fraction of the total cell area. In this regard, adding Al_2O_3 into the substrate is an effective strategy to achieve high cell performance within a fixed dimension.

4. Conclusions

The influence of reduced substrate shunting current on cell performance of IP-SOFCs was investigated. The resistivity of substrates was tailored by adding Al_2O_3 into the PSZ substrates. Variation in the resistivity follows the mixture rules of composites in which insulating phases are dispersed in a continuous conducting matrix. The strategy to add Al_2O_3 into PSZ was effective for reducing shunting current flow through the substrate. As the amount of Al_2O_3 addition was increased, the power output of the cell was enhanced due to reduced shunting current, especially in the case of narrow cell-to-cell gap distance. If the amount of Al_2O_3 addition was greater than 26 vol%, however, Ni from the anode migrated to react with Al_2O_3 in the PSZ substrate, which resulted in performance degradation. Reduced shunting currents achieved through Al_2O_3 addition improved the power densities of two-cell arrayed IP-SOFC by 30%.

Acknowledgement

This work was supported by a National Research Foundation of Korea grant funded by the Korean Government (MEST) (2009-0093454).

References

[1] F.J. Gardner, M.J. Day, N.P. Brandon, B.N. Pashley, M. Cassidy, SOFC technology development at Rolls-Royce, J. Power Sources 86 (2000) 122–129.
[2] T.S. Lai, J. Liu, S.A. Barnett, Effect of cell width on segmented-in-series SOFCs, Electrochem. Solid-State Lett. 7 (2004) A78–A81.
[3] T.S. Lai, S.A. Barnett, Design considerations for segmented-in-series fuel cells, J. Power Sources 147 (2005) 85–94.
[4] T.S. Lai, S.A. Barnett, Effect of cathode sheet resistance on segmented-in-series SOFC power density, J. Power Sources 164 (2007) 742–745.
[5] P.K. Srivastava, T. Quach, Y.Y. Duan, R. Donelson, S.P. Jiang, F.T. Ciaacchi, Electrode supported solid oxide fuel cells prepared by DC magnetron sputtering, Solid State Ionics 99 (1997) 311–319.
[6] T. Tsai, E. Perry, S.A. Barnett, Low-temperature solid-oxide fuel cells utilizing thin bi-layer electrolytes, J. Electrochem. Soc. 144 (1997) L130–L132.
[7] M.R. Pillai, D. Gostovic, I. Kim, S.A. Barnett, Short-period segmented-in-series solid oxide fuel cells on flattened tube supports, J. Power Sources 163 (2007) 960–965.

[8] Y.-B. Kim, S.-J. Ahn, J. Moon, J. Kim, H.-W. Lee, Direct-write fabrication of integrated planar solid oxide fuel cells, J. Electroceram. 17 (2006) 683–687.
[9] H. Luhleich, J. Dias, H. Nickel, The coat-mix procedure using carbon fillers, Carbon 35 (1997) 95–102.
[10] W.D. Kingery, H.K. Bowen, D.R. Uhlmann, Introduction to Ceramics, second ed., John Wiley & Sons, New York, 1976.
[11] J.N. Roelofsen, R.C. Peterson, Structural variation in nickel aluminate spinel, Am. Miner. 77 (1992) 522–528.
[12] R. O'Hayre, S.W. Cha, W. Colella, F.B. Prinz, Fuel Cell Fundamentals, second ed., John Wiley & Sons, New York, 2006.
[13] R.M. German, Particle Packing Characteristics, Metal Powder Industries Federations, New Jersey, 1989.